

Effect of Nb and Ti on Corrosion Characteristics of Low Alloy Steel in Supercritical CO₂ Environment

Hongwei Wang^{1,*}, Hongyan Wang², Xiuhua Gao², Chi Yu^{3,4}

¹ School of Control Engineering, Northeastern University at Qinhuangdao, Qinhuangdao 066004, China;

² The State Key Laboratory of Rolling and Automation, Northeastern University, Shenyang 110819, China;

³ School of Resources and Materials, Northeastern University at Qinhuangdao, Qinhuangdao 066004, China;

⁴ School of Mechanical Engineering, Yanshan University, Qinhuangdao 066000, China

*E-mail: wanghw0819@163.com

Received: 2 February 2019 / Accepted: 21 April 2019 / Published: 29 October 2019

The immersion test and electrochemical experiment are performed to investigate the influence micro-alloying elements Nb and Ti on corrosion characteristics of low alloy steel exposed to CO₂ saturated saline solution environment. The corrosion kinetics, potentiodynamic polarization, surface morphology, corrosion phases and max pitting depth are studied deeply and thoroughly. The results show that the major corrosion phases are FeCO₃, the corrosion rate of No.2 steel with micro-alloying elements Nb and Ti is lower than that of steel No.1, and showing the good corrosion resistance.

Keywords: low alloy steel; CO₂ environment; corrosion characteristics; potentiodynamic polarization

1. INTRODUCTION

The pipeline steel often suffer corrosion in the oil and gas industry, which would result in serious damage and great economic loss [1-5]. The low alloy steel is the most widely used pipeline steel due to low cost. The corrosion property of low alloy steel exposed to CO₂ is a very complex because the formation water and the carbon dioxide will lead to the pipeline failure, the candidate materials is difficult issues containing economy and safety. So it is the most intractable problem to study the corrosion characteristics of low alloy steel exposed to CO₂ saturated saline environment.

The CO₂ corrosion problems of low alloy steel have attracted more attention, and researchers have obtained some results [6-10]. Generally, corrosion layers would influence corrosion characteristic, so it is important to study the stability of layer structure. Wu et al have studied the property of the

surface film formed on N80 steel for 72 h at 80°C with a carbon dioxide partial pressure 0.5 MPa, the surface film is composed of unstable precipitated FeCO_3 [11]. Zhang et al have investigated the initial surface layers of 20-steel and 3-Cr steel, the corrosion products are FeCO_3 and FeO , and further analyze underlying mechanism[12]. Pfenning et al have studied the effects of alloy element Cr on corrosion resistance under CO_2 environment[13]. The effects of CO_2 and pressure on corrosion behavior of steels with different amounts of chromium are also investigated [14]. Cui and Ko et al have revealed the influences of temperature on corrosion rate by studying corrosion products[15-16]. Nazari et al have investigated the effects of temperature and pH on corrosion resistance of X70 pipeline steel and get the better conditional parameters for the formation of corrosion product film [17]. Also corrosion properties with long immersion time are researched under the CO_2 environment, the corrosion product and corrosion film play an important role[18-19]. It is found that many scholars have investigated the effect of some factors including pressure, chromium, temperature, pH and immersion time on the corrosion resistance, but the effect micro-alloying additions of Nb and Ti on corrosion characteristics of low alloy steel immersed in CO_2 environment is seldom reported. Nb and Ti have been proved to be efficient in improving the corrosion resistance of low alloy steel under various aggressive medium environments, the researchers have not get a general conclusion [20-21].

Obviously, it is meaningful to know the properties of the surface film induced from CO_2 corrosion, and obtain the influence of specific parameters on corrosion behavior. In this paper, the effects micro-alloying Nb and Ti on the corrosion behavior of low alloy steel immersed in water-saturated supercritical CO_2 environment with long immersion time are studied. The corrosion characteristics are systematically studied in term of the corrosion model, corrosion morphology and corrosion products, which will provide great value in oil and gas field.

2. EXPERIMENTAL

2.1 Material and sample preparation

The experimental steels are developed in laboratory and the chemical compositions are shown in Table 1. They are achieved by smelting technology in a vacuum induction furnace. It is then forged into slabs, and reheated at 1200°C for 2 h, and rolled into the plates by thermo-mechanical control process (rolling temperature for 850°C and 841 °C, final cooling temperature for 660 °C and 645 °C and cooling rate for 9.7 °C /s and 10.3 °C /s), marked as No.1 and No.2, respectively. The specimens are cut into 20 mm × 25 mm × 4 mm for immersion test. The electrochemical samples are machined into 10 mm × 10 mm × 4 mm, and the area of exposure to the electrolyte is 100 mm², other surfaces are isolated by epoxy resin. All the specimens are ground up 1200 grit using silicon carbide paper. The distilled water and ethanol are used to dust and grease, and dried by nitrogen. The samples are weighted by balance with very high precision of 0.01mg and stored in a moisture-free desiccator.

Table 1. Chemical components of experimental steels (mass percent, %)

	C	Mn	Si	P	S	Al	Nb	Ti
No.1	0.16	1.38	0.32	0.012	0.009	0.030	—	—
No.2	0.15	1.36	0.30	0.013	0.009	0.030	0.05	0.03

2.2 Immersion tests

Immersion tests are performed in a high temperature and high pressure autoclave with 5 L volume, the schematic diagram is displayed in Fig.1. The test solution is 3.5 wt% NaCl. First, all specimens are placed in the autoclave, and then sealed. The temperature is at 75°C. Then N₂ is injected into the solution for 2 h to deoxygenate. Third, the mixed gas is infused into the electrolyte until the total pressure is 1.2 MPa (0.64 MPa CO₂ and 0.56 MPa N₂). The corrosion characteristics of low alloy steel after 24 h, 48 h, 96 h, 192 h, 288h and 384h are researched. After corrosion test, the samples are taken out, and the deionized water and alcohol are used to dust and grease, and dried by nitrogen. The corrosion scale is removed by the chemical cleaning method [22]. Based on the ASTM G1-03 standard, the corrode samples are rinsed, dried and then weighted again. The corrosion rate is calculated using the following equation.

$$v = \frac{8.76 \times 10^4 \times (W_1 - W_2)}{S \times T \times \rho} \tag{1}$$

where v is the corrosion rate (mm/year), W_1 and W_2 are the start and end weight of sample (g), respectively, S is the surface area (cm²), T is the corrosion time (h), ρ is the physical density of low alloy steel.

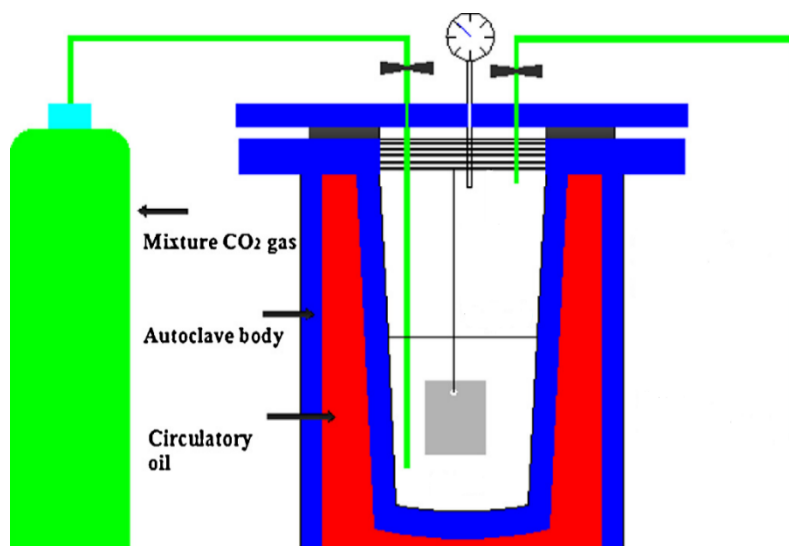


Figure 1. Structure schematic of autoclave setup

2.3 Electrochemical measurements

The electrochemical experiments are performed using a conventional three-electrode cell, the

Pt-plated electrode as the auxiliary electrode, the saturated calomel electrode (SCE) as the reference electrode, and the test steel as the working electrode. The polarization curves are conducted at a scanning rate of 0.1 mV/s. The measurements are performed in aerated 3.5 wt% NaCl containing mixed gas CO₂ and N₂, the electrolyte temperature is kept at 75 °C.

2.4 Morphology observation

The corrosion morphologies of low alloy steel are observed using scanning electron microscope (SEM). The corrosion phases are detected by X-ray diffraction (XRD) with CuK α radiation, and the phases analysis are carried out by matching peak positions automatically with MDI Jade software. The max pitting depth of test material is acquired by 3D microscope outfitted with a laser for precision dissection.

3. RESULTS AND DISCUSSION

3.1 Corrosion kinetics

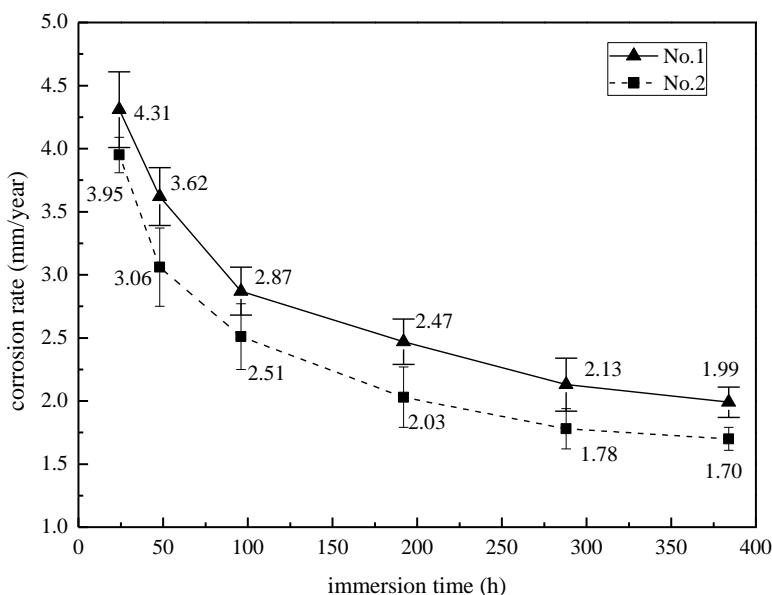


Figure 2. The corrosion kinetics curve of experimental steels in CO₂ environment at 75°C after immersion for 24 h, 48 h, 96 h, 192 h, 288 h and 384 h

The corrosion rates of low alloy steel with immersion time are shown in Fig.2. The average corrosion rates of No.1 and No.2 steels after 384 h immersion are 1.99 mm/y and 1.70 mm/y, respectively, which show No.2 steel has good corrosion resistance. It is seen that the corrosion rates of two steels after immersion 24 h are high. With the increase of the immersion time, the corrosion rates decrease. After 284 h immersion, the corrosion rates reach to a stable level, which may be due to the

dense and thick layer has formed on the steel surface. Our tests show the similar results with Ref [18], it indicates the corrosion data are correct. The corrosion rate of No.2 steel is lower than that of No.1 during the entire corrosion process, which may be result from the role of micro-alloying additions of Nb and Ti.

3.2 Potentiodynamic polarization

The polarization curves of No.1 and No.2 steels after immersion 24 h, 48 h, 96 h, 192 h, 288 h and 384h are indicated in Fig. 3. The fitting values of corresponding electrochemical corrosion parameters such as anodic Tafel constants (b_a), cathodic Tafel constants (b_c), corrosion potential (E_{corr}), and corrosion current density (I_{corr}) are listed in Table 2.

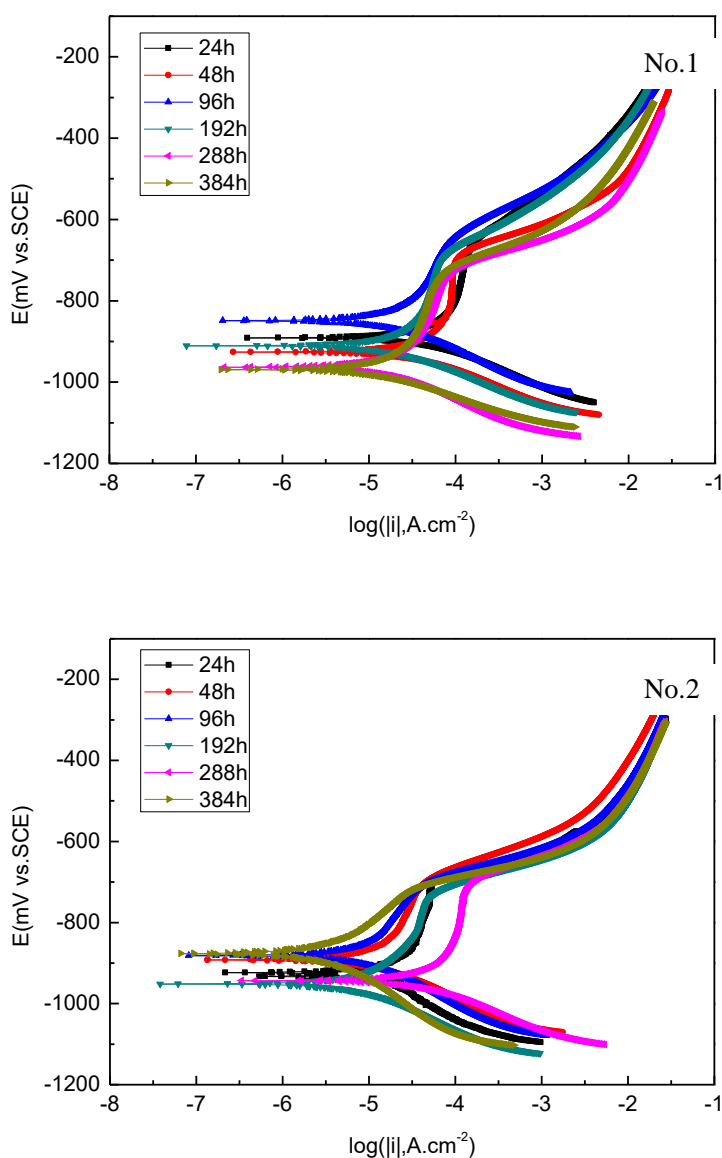


Figure 3. Potentiodynamic polarization curves of experimental steels in CO₂ environment at 75°C after immersion for 24 h, 48 h, 96 h, 192 h, 288 h and 384 h

It is seen that the change of the cathodic Tafel constants is very small with the increase the immersion time, and anodic Tafel constants vary greatly. The anode polarization curves underwent a slow rise in current, which is the characteristic of passivation, it is possible that a relatively dense corrosion layer is formed. Then the current increases, which may be due to the destruction of the corrosion layer.

Table 2. Potentiodynamic polarization parameters from a curve-fitting approach

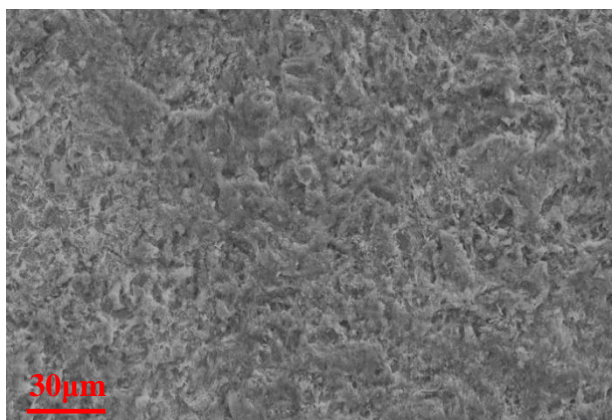
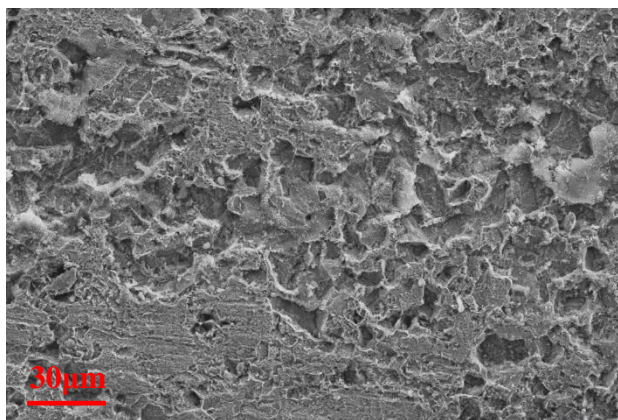
sample	Immersion time/hour	b_a (mV/dec)	b_c (mV/dec)	E_{corr} (mV vs.SCE)	I_{corr} (mA.cm ⁻²)
No.1	24	770	-110	-891	0.0838
	48	591	-1021	-926	0.0586
	96	5391	-123	-849	0.0347
	192	514	-103	-910	0.0311
	288	425	-125	-963	0.0288
	384	352	-81	-969	0.0194
No.2	24	573	-107	-943	0.0704
	48	747	-123	-892	0.0213
	96	362	-128	-881	0.0121
	192	244	-117	-951	0.0113
	288	144	-94	-924	0.0065
	384	218	-178	-876	0.0058

It is found that the corrosion properties of two steels are very similar and exhibit two stages from Table 2. At the first stage(24 h-96 h), the corrosion current density decreases quickly, the change values are 0.0491 mA/cm² and 0.0583 mA/cm², respectively. At the second stage (192 h-384 h), the corrosion current density varies small, the change values are 0.0117 mA/cm² and 0.0055 mA/cm², respectively. These show that the No.1 and No.2 steels have good corrosion resistance at later stage, which might be the formation of dense and thick corrosion layer, and can effectively protect the steel substrate. As a whole, the corrosion current density of No.2 steel is much smaller than one of No.1 steel at each stage, the smallest corrosion current density is seen at 384 h of No.2, only 0.0058 mA/cm², which may be result from the role of micro-alloying additions of Nb and Ti.

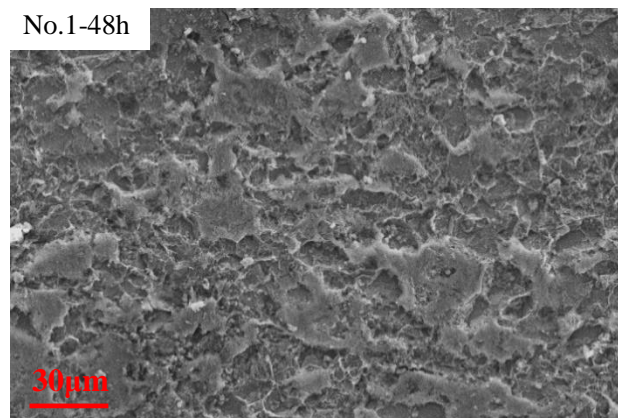
3.3 Surface morphologies and composition analysis of corrosion product

The microscopic morphologies of low alloy steel after different immersion time are shown in Fig.4. Obviously, at the early stage, the corrosion products are irregular, on the contrary, at the later stage, the corrosion products are regular and compact. The typical XRD results are used to identify and characterize the corrosion phase, as indicated in Fig. 5. The corrosion products are mainly FeCO₃ by the diffraction angles of peaks. Fe is observed when the test steels are immersed for 24h, it is found that there are some gaps combining with microscopic morphologies, which is possible to be passages that the corrosion solution diffuses into the inner layer and even into the substrate surface, these will cause the poor corrosion resistance. The nucleation process of FeCO₃ is affected by stochastic variations of the ion concentration, resulting in an irregular formation at immersion 48h and 96 h. At

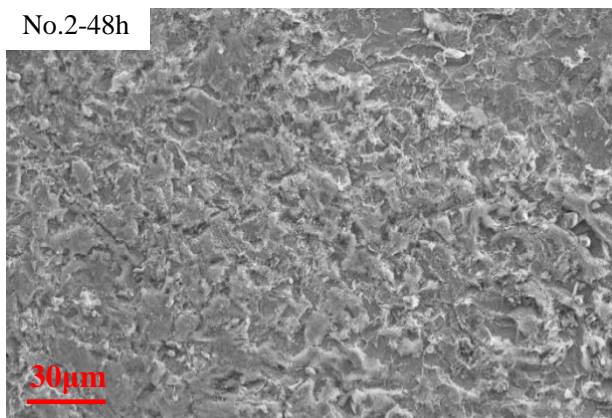
the later stage, Fe are not observed, and the number of FeCO_3 crystals characteristic peak becomes larger with immersion time, the corrosion products are dense, the more FeCO_3 crystals are formed on sample surfaces, and protect the steel matrix, the No.2 steel is significantly larger than No.1, it reveals No.2 has good corrosion resistance, which is in accordance with corrosion rate and surface morphology described above.



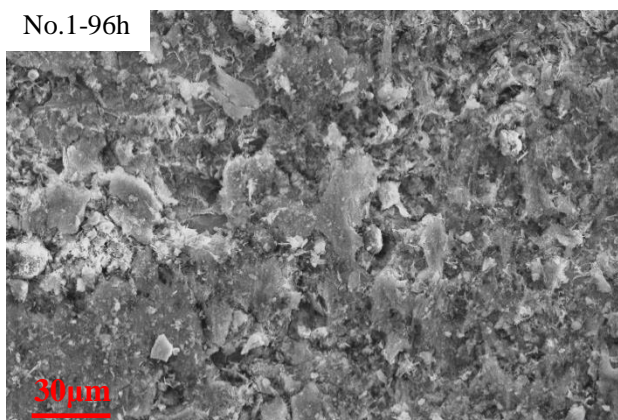
No.1-48h



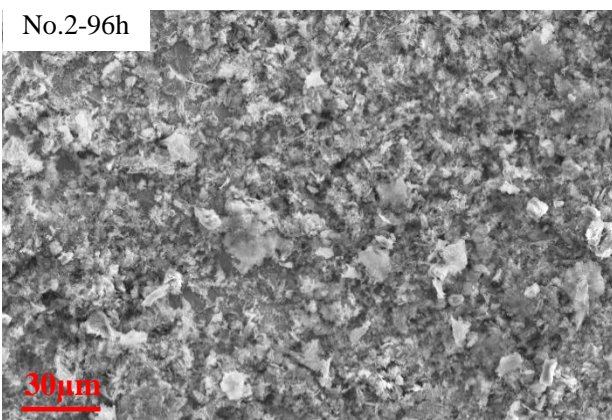
No.2-48h



No.1-96h



No.2-96h



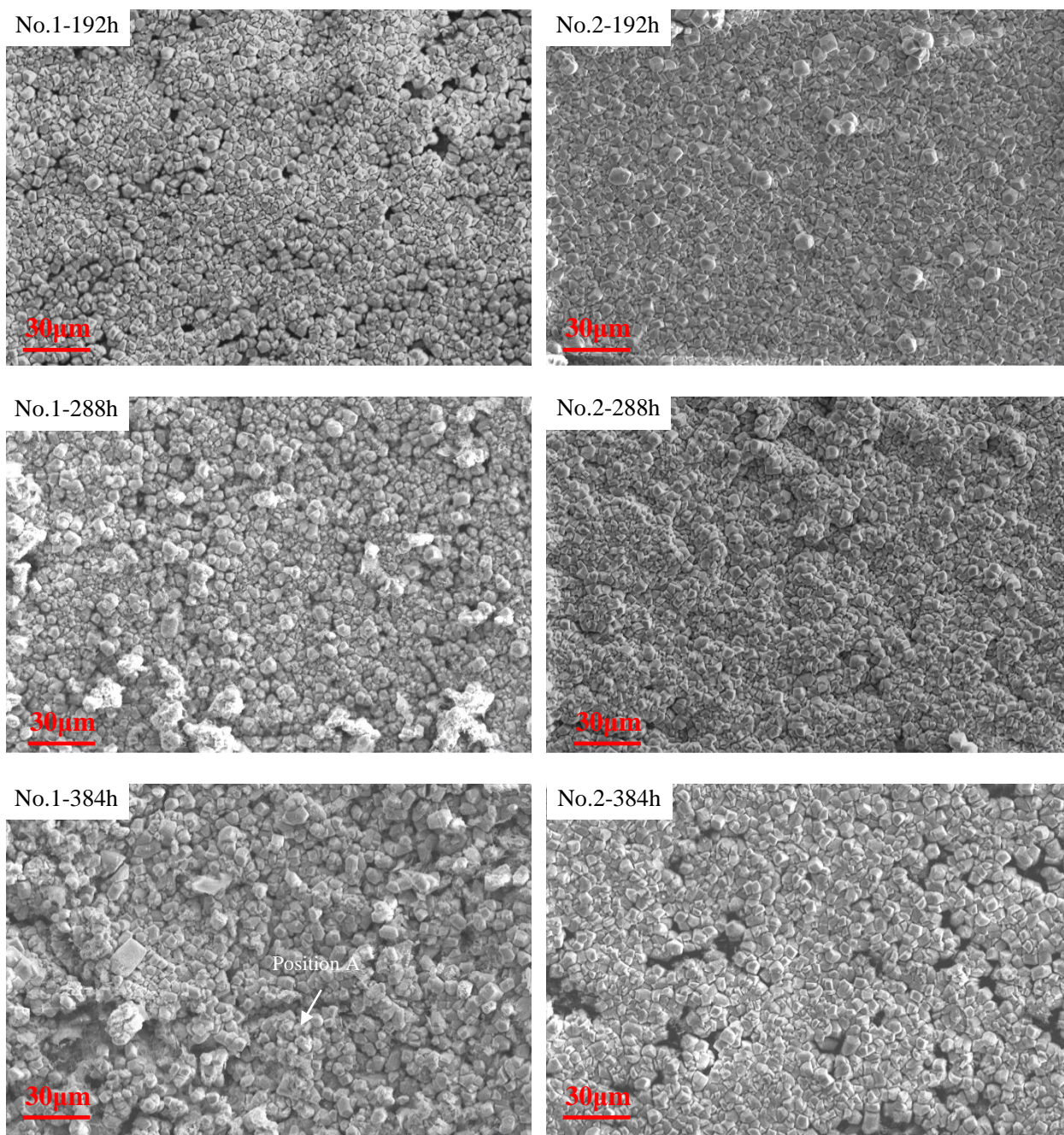


Figure 4. SEM images of corroded surface for experimental steels in CO₂ environment at 75°C after immersion for 24 h, 48 h, 96 h, 192 h, 288 h and 384 h

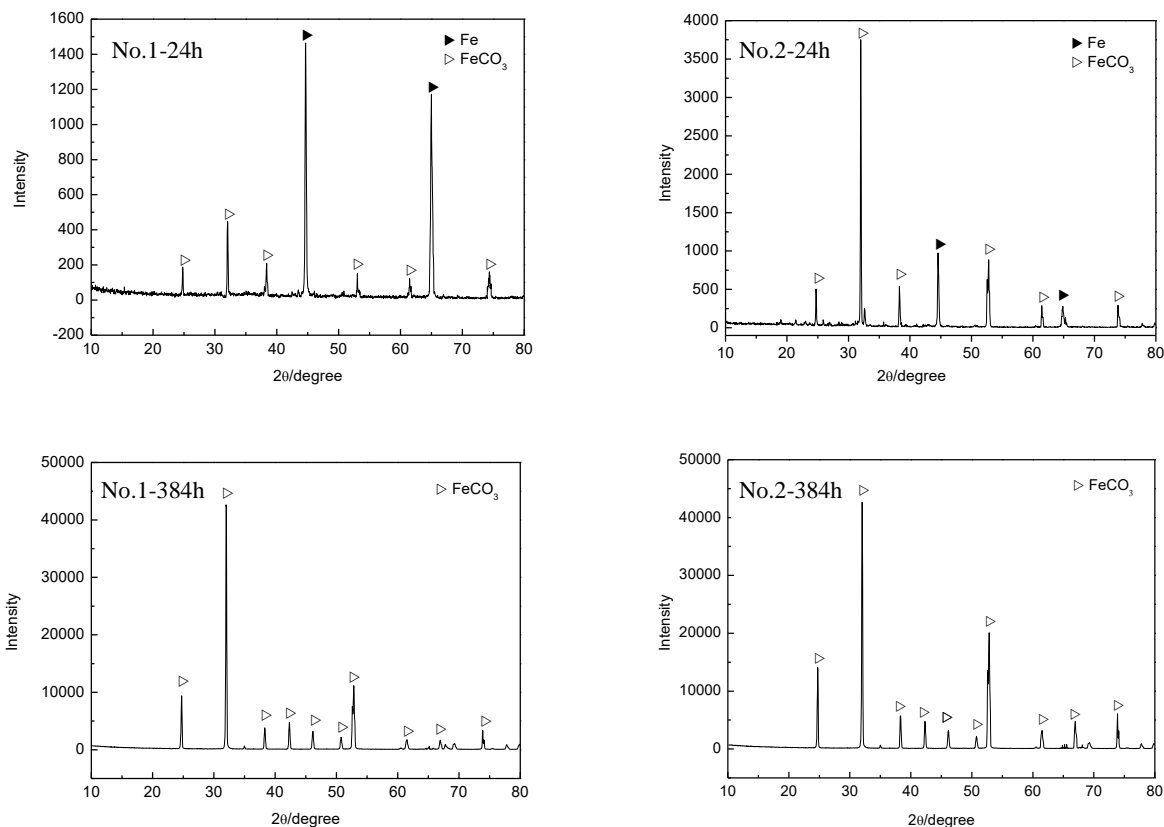
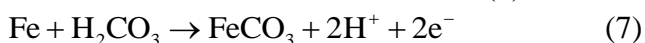
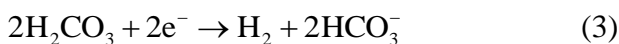


Figure 5. The typical XRD of experimental steels in CO₂ environment at 75°C after immersion 24h and 384h

As we know, when injecting CO₂ into the saline water, the dissolved CO₂ molecules hydrates to form carbonic acid and establish a corrosive environment [23]. The electrochemical reaction of low alloy steel are very complex under CO₂ environment. It mainly includes the cathodic reaction and the anodic reaction, the details are shown as follows[24].



The pH changes from 4.6 to 4.9 with the increase of immersion time, the similar experiments are done and the results are almost identical with Ref [25]. The change of pH would not affect cathodic reaction by equations (3) and (4), this result is consistent with the result of polarization curve, the cathodic Tafel constants vary very small.

The max depth of the corrosion pit on the steel surface changes with the corrosion environment and immersion time, which is one of the important data for characterizing the corrosion phenomenon. Yu and Hatami et al have studied the corrosion kinetics by establishing mathematical model about the

average corrosion rate [26-27]. But it is known that the research of max pitting depth is of great significance, and few studies are reported. The max depth of pitting holes for steels No.1 and No.2 after different immersion time are shown in Table 3. And the typical three-dimensional graphics of the film that desquamated the surface are indicated in Fig.6. The depth of No. 1 steel is obviously higher than that of No. 2 steel, which indicate that No. 2 steel has better corrosion resistance, and is consistent with the previous analysis results.

Table 3. The max pitting depth of No.1 and No.2 steels in CO₂ environment at 75°C after different immersion time (μm)

	24h	48h	96h	192h	288h	384h
No.1	40.6	56.9	80.3	94.7	109.8	123.9
No.2	30.1	48.6	60.5	74.3	88.6	99.0

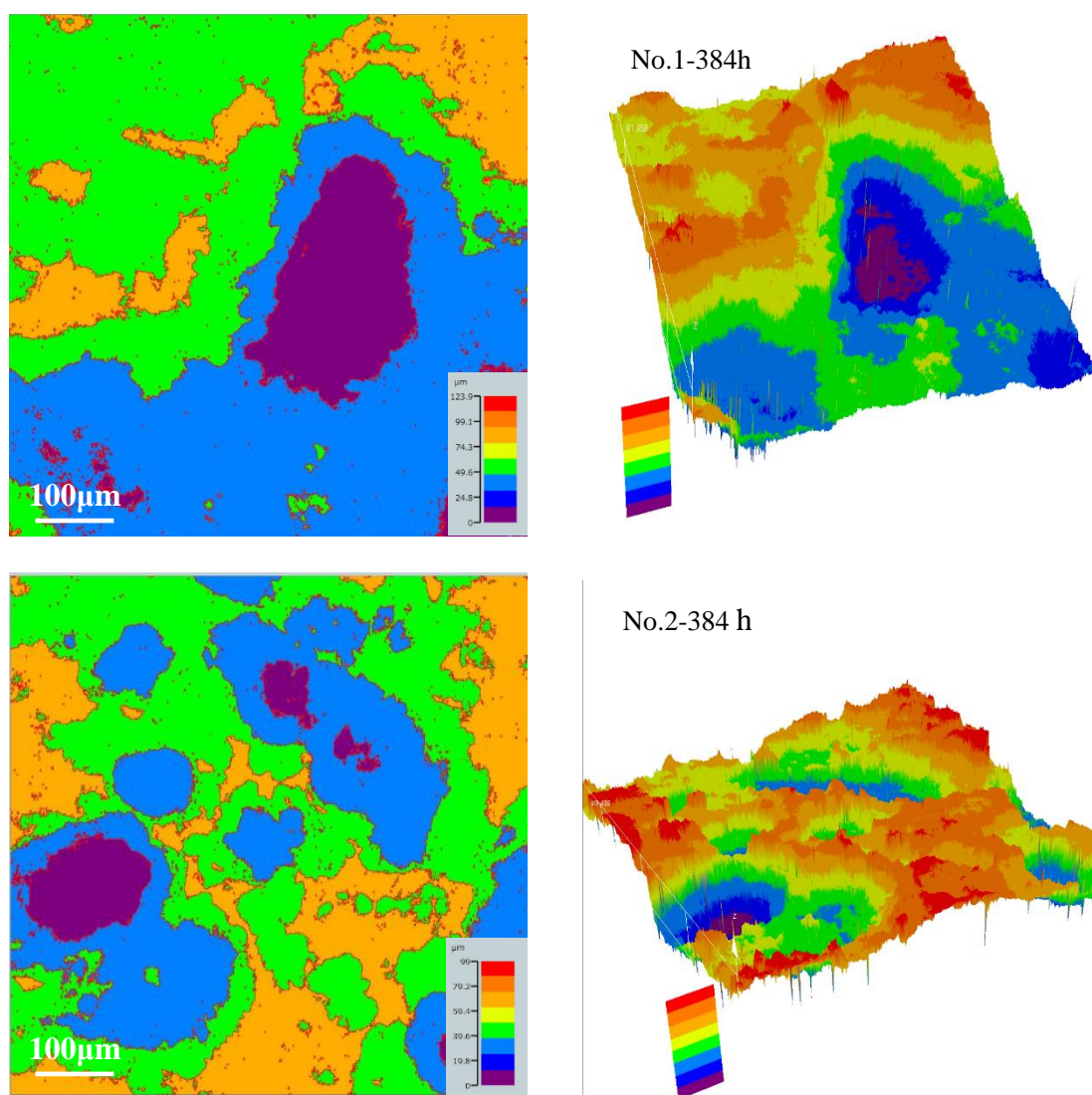


Figure 6. Three-dimensional images of corroded surface for No.1 and No.2 steels in CO₂ environment at 75°C after immersion 384 h

It is found that the relationship of the corrosion depth (H) and immersion time (t) satisfy the following exponential equation from the above date.

$$H = k_1 \times e^{\alpha t} + k_2 \times e^{\beta t} \tag{8}$$

where k_1, k_2, α, β are undetermined coefficient.

The fitting parameters are shown in Table 4 using curve fitting tool in MATLAB.

Table 4. The fitting parameters of mathematical model for max pitting depth and immersion time

	k_1	α	k_2	β
No.1	76	0.001281	-66	-0.02291
No.2	56	0.001536	-62	-0.03397

To further validate the effect of fitting dates, the relative residual error can be given as follows.

$$\eta = \left(\frac{v_{exp} - v_{fit}}{v_{exp}} \right) \times 100\% \tag{9}$$

where v_{exp} and v_{fit} are measured from the experimental and fitting, respectively.

Fig.7 shows the relative residual errors of No.1 and No.2 steels. It is seen that the errors are within 3%. Residual error is most frequently used to estimate the fitting effect, the 3% error shows a good fitting effect, these data indicate the choice of the exponential equation is reasonable. Thus, it can well predict the corrosion depth of low alloy steel, this study would provide the knowledge for the oil and gas industry.

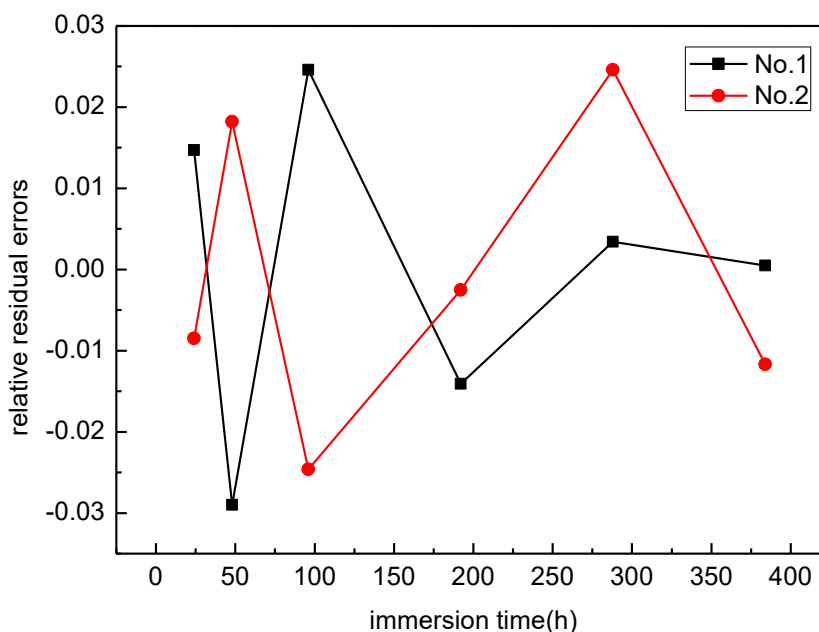


Figure 7. The curves of relative residual error for low alloy steel

4. CONCLUSIONS

The corrosion properties of low alloy steel with long immersion time are studied under CO₂ environment. The results indicate that the corrosion current density of low alloy steel decreases with immersion time, the corrosion current density of No.2 steel is much smaller than one of No.1 steel. The corrosion process includes two stages: Stage I, the irregular corrosion product FeCO₃ is formed, and Fe is observed; Stage II, the growth of FeCO₃ controls the corrosion phase, the number of FeCO₃ crystals characteristic peak becomes larger with immersion time, the dense and compact corrosion products are formed on the surface, and can effectively protect steel substrate. Combing with microscopic morphologies, weight loss and corrosion depth, the corrosion resistance of No.2 steel is better than that of No.1 steel, which show micro-alloying additions of Nb and Ti plays an important role.

ACKNOWLEDGMENT

This work was supported by the China Postdoctoral Science Foundation (No.2018M631761), the Nature Science Foundation of Liaoning Province (No.20170540310), the Fundamental Research Funds for the Central Universities (No. N182303030), the Higher Educational Science and Technology Program of Hebei Province (No.QN2019317) and the Natural Science Foundation of China (No.61903072).

References

1. S. Nešić, *Corros. Sci.*, 49 (2007) 4308.
2. J. L. Tang, Y. X. Hu, H. Wang, Y. Q. Zhu, Y. Wang, Z. Nie, Y. Y. Wang, B. Normand, *Int. J. Electrochem. Sci.*, 14 (2019) 2246.
3. O. Yevtushenko, D. Bettge, R. Bassler, S. Bohraus, *Mater. Corros.*, 66 (2015) 334.
4. Q. Qiao, G. X. Cheng, W. Wu, Y. Li, H. Huang, Z. F. Wei, *Eng. Fail. Anal.*, 64 (2016) 126.
5. C. W. Shi, Y. B. Zhang, P. Liu, Y. L. Xie, *Int. J. Electrochem. Sci.*, 13 (2018) 2412.
6. H. Mansoori, D. Young, B. Brown, M. Singer, *J. Nat. Gas Sci. Eng.*, 59 (2018) 287.
7. M. Javidi, S. Bekhrad, *Eng. Fail. Anal.*, 89 (2018) 46.
8. J. Miao, J. T. Yuan, Y. Han, X. Q. Xu, *Rare Metal Mat. Eng.*, 47 (2018) 1965.
9. W. Liu, J. J. Dou, S. L. Lu, P. Zhang, Q. H. Zhao, *Appl. Surf. Sci.*, 367 (2016) 438.
10. L. Wei, K. W. Gao, Q. Li, *Appl. Surf. Sci.*, 440 (2018) 524.
11. S. L. Wu, Z. D. Cui, F. He, Z. Q. Bai, S. L. Zhu, X. J. Yang, *Mater. Lett.*, 58 (2004) 1076.
12. J. Zhang, Z. L. Wang, Z. M. Wang, X. Han, *Corros. Sci.*, 65(2012)397-404.
13. A. Pfennig, R. Bassler, *Corros. Sci.*, 51 (2009) 931.
14. A. Pfennig, A. Kranzmann, *Corros. Sci.*, 65 (2012) 441.
15. Z. D. Cui, S. L. Wu, S. L. Zhu, *Appl. Surf. Sci.*, 252 (2006) 2368.
16. M. Ko, B. Ingham, N. Laycock, *Corros. Sci.*, 80 (2014) 237.
17. M. H. Nazari, S. R. Allahkaram, M. B. Kermani, *Mater. Design*, 31 (2010) 3559.
18. Z. G. Liu, X. H. Gao, J. P. Li, *Electrochim. Acta*, 213 (2016) 842.
19. Z. G. Liu, X. H. Gao, L. X. Du, J. P. Li, Y. Kuang, B. Wu, *Appl. Surf. Sci.*, 351 (2015) 610.
20. H. Ali-Loytty, M. Hannula, M. Honkanen, K. Ostman, K. Lahtonen, M. Valden, *Corros. Sci.*, 112 (2016) 204.
21. L. Weng, L. X. Du, H. Y. Wu, *Int. J. Electrochem. Sci.*, 13 (2018) 5888.
22. Z. G. Liu, X. H. Gao, L. X. Du, J. P. Li, P. Li, *Mater. Corros.*, 67 (2016) 817.
23. S. Q. Guo, L. N. Xu, L. Zhang, W. Chang, M. X. Lu, *Corros. Sci.*, 110 (2016) 123.
24. M. Nordsveen, S. Nesic, R. Nyborg, A. Stangeland, *Corrosion*, 59 (2003) 443.

25. S. Q. Guo, L. N. Xu, L. Zhang, *Corros. Sci.*, 63 (2012) 246.
26. C. Yu, X. H. Gao, H. W. Wang, *Mater. Lett.*, 209 (2017) 459.
27. S. Hatamia, A. Ghaderi-Ardakania, M. Niknejad-Khomamib, F. Karimi-Malekabadic, M. R. Rasaeia, A. H. Mohammadid, *J. Supercrit. Fluid.*, 117 (2016) 108.

© 2019 The Authors. Published by ESG (www.electrochemsci.org). This article is an open access article distributed under the terms and conditions of the Creative Commons Attribution license (<http://creativecommons.org/licenses/by/4.0/>).